Mechanism of Glomerulotubular Balance in the Setting of Heterogeneous Glomerular Injury

PRESERVATION OF A CLOSE FUNCTIONAL LINKAGE BETWEEN INDIVIDUAL NEPHRONS AND SURROUNDING MICROVASCULATURE

I. ICHIKAWA, J. R. HOYER, M. W. SEILER, and B. M. BRENNER, *Laboratory of Kidney and Electrolyte Physiology and Departments of Medicine and Pathology, Brigham and Women's Hospital, Children's Hospital Medical Center, West Roxbury Veterans Administration Hospital, and Harvard Medical School, Boston, Massachusetts 02115*

ABSTRACT Autologous immune complex nephropathy (AICN), an experimental model for human membranous glomerulopathy, is characterized by marked heterogeneity in function from glomerulus to glomerulus. However, the fraction of the filtered load of fluid reabsorbed by the proximal tubule remains nearly constant from nephron to nephron, despite wide variation in single nephron glomerular filtration rate (SNGFR). To define the physiological mechanisms responsible for this marked variation in SNGFR values within a given kidney and for the remarkable preservation of glomerulotubular balance, the various determinants of fluid exchange across glomerular and peritubular capillary networks were evaluated in Munich-Wistar rats with AICN. For comparison, similar measurements were obtained in rats with the functionally more homogeneous lesion of heterologous immune complex nephropathy. In AICN rats studied ~5 mo after injection of renal tubule epithelial antigen (Fx1A), a high degree of glomerulus-proximal tubule balance was found, despite marked variations in SNGFR values within a single kidney. These changes were associated with marked heterogeneity in immunoglobulin and complement deposition within and among glomeruli. Although mean capillary hydraulic pressure and Bowman's space hydraulic pressure ranged widely from glomerulus to glomerulus, the mean glomerular transcapillary hydraulic pressure difference was remarkably uniform among these functionally diverse glomeruli and could not, therefore, be implicated as the cause of the dispersion in SNGFR values. The two remaining determinants of SNGFR, namely, glomerular plasma flow rate (Q_A) and ultrafiltration coefficient (K_f), varied markedly from glomerulus to glomerulus, but always in direct proportion to SNGFR, and proved to be responsible for the marked variation in SNGFR.

The mean net peritubular capillary reabsorptive force ($\bar{P}_r$) correlated closely with the absolute rate of fluid reabsorption in adjacent proximal tubules (APR) in AICN. Of the factors determining $\bar{P}_r$, peritubular capillary hydraulic pressure was essentially constant in a given AICN kidney, whereas peritubular capillary plasma protein concentration and oncotic pressure varied directly with APR and largely accounted for the observed tight correlation between $\bar{P}_r$ and APR.

On the basis of these observed correlations, we suggest that the close quantitative coupling between SNGFR and APR in individual nephrons in AICN is due to the functional response of individual glomeruli: those with the most pronounced declines in SNGFR are characterized by the most pronounced declines in Q_A and K_f. The resultant low peritubular capillary

Portions of these studies were presented at the annual meetings of the American Federation for Clinical Research, Wash., D. C., 17 May, 1979; Society for Pediatric Research, San Antonio, Tex., 2 May 1980; and American Society for Clinical Investigation, Wash., D. C., 11 May 1980, and have been published in abstract form.

Received for publication 23 February 1981 and in revised form 2 September 1981.

oncotic pressure favors a decline in APR, thus favoring nearly perfect glomerulotubular balance. In glomeruli with higher SNGFR values, Q_A and K_f values are also higher. These changes in K_f once again are capable of establishing the conditions in downstream peritubular capillaries, this time favoring augmented APR (i.e., high intracapillary oncotic pressure), again leading to nearly perfect glomerulotubular balance.

INTRODUCTION

Membranous glomerulopathy is a common cause of the nephrotic syndrome in man. The model of autologous immune complex nephropathy, or AICN, has long been employed by investigators to characterize the morphological and immunological components of this lesion in animals (1–4). Allison et al. (5) have recently demonstrated marked heterogeneity of function from glomerulus to glomerulus in a given kidney in AICN. These workers observed, however, that absolute proximal fluid reabsorption rate (APR) also varied widely from nephron to nephron in AICN but that reabsorption remained proportional to single nephron glomerular filtration rate (SNGFR), so that a high degree of glomerulotubular balance was maintained for each nephron unit. The present study was undertaken to further evaluate the basis for this close coupling between SNGFR and APR in AICN by quantifying the specific determinants of filtrate formation and proximal fluid reabsorption in paired nephron-peritubular capillary units. For comparison, control rats and rats with the more uniform lesion of heterologous immune complex glomerulopathy (HICN) were studied.

GLOSSARY

$\overline{AP}$	Mean femoral arterial pressure, *mm Hg*
AICN	Autologous immune complex nephropathy (active Heymann nephritis)
APR	Absolute proximal reabsorption rate, *nl/min*
BW	Body weight, *g*
C	Protein concentration, *g/dl*
C_{IN}	Whole kidney inulin clearance, *ml/min*
GBM	Glomerular basement membrane
Hct	Blood hematocrit in femoral artery, *vol %*
HICN	Heterologous immune complex nephropathy (passive Heymann nephritis)
K_f	Glomerular capillary ultrafiltration coefficient, *nl/(s · mm Hg)*
K_r	Peritubular capillary reabsorption coefficient, *nl/(s · mm Hg)*
KW	Kidney weight, *g*
P	Hydraulic pressure, *mm Hg*
P_r	Local net peritubular transcapillary reabsorptive pressure, *mm Hg*
ΔP	Glomerular or peritubular transcapillary hydraulic pressure difference, $P_{GC} - P_T$ or $P_C - P_I$, *mm Hg*
Π	Colloid osmotic pressure, *mm Hg*
$\Delta\Pi$	Peritubular transcapillary colloid osmotic pressure difference, $\Pi_C - \Pi_I$, *mm Hg*
Q	Plasma flow rate, *nl/min*
R	Resistance to blood flow, *dyn · s · cm*$^{-5}$
SNFF	Single nephron filtration fraction
SNGFR	Single nephron glomerular filtration rate, *nl/min*
$(TF/P)_{In}$	Late proximal tubule fluid-to-plasma inulin concentration ratio
$U_{alb}V$	Urinary albumin excretion rate, *mg/d per two kidneys*

Overbar

$\bar{}$	Mean value

Subscripts

A	Afferent arteriole
C	Peritubular capillary
C^1	Distal-most surface branches of peritubular capillaries
E	Efferent arteriole
GC	Glomerular capillary
I	Cortical interstitium
T	Proximal tubule

METHODS

Induction of immune complex nephropathy

AICN was induced in 1-mo-old Munich-Wistar rats by intradermal injection of 0.2 ml of an emulsion prepared by sonication of equal volumes of complete Freund's adjuvant (Difco Laboratories, Detroit, Mich.) and a suspension of 0.15 M saline containing 40 mg/ml of rat proximal tubule epithelial antigen Fx1A. Fx1A was isolated from Sprague-Dawley rat renal cortices in the manner described by Edgington et al. (1) and lyophilized before use. At the time of injection, rats also received a subcutaneous injection of 0.1 ml of pertussis vaccine containing 2×10^{10} organisms/ml. Some rats received a second intradermal injection of 4 mg of Fx1A in emulsion (prepared as described above) 1–2 mo later. Animals were subjected to study at 5–6 mo of age.

Heterologous immune complex nephropathy (HICN) was induced in 15-mo-old Munich-Wistar rats by a single intravenous injection of 1 ml of sheep antiserum to Fx1A. The antiserum to Fx1A was obtained after twice-monthly intramuscular injection of rat Fx1A into an adult female sheep. The initial injection contained 40 mg of Fx1A in complete Freund's adjuvant, and subsequently 20 mg of Fx1A was injected after sonication with incomplete Freund's adjuvant. The antisera used in these studies were obtained 1 wk after the seventh injection of Fx1A. 2 wk later animals were subjected to study.

1–2 d before study, 24-h urine collections were obtained for determination of albumin excretion rate by an immunodiffusion method (6). In all studies to be described, values obtained in AICN and HICN animals were compared with those from age-matched normal Munich-Wistar rats.

Micropuncture studies

General procedure. Animals were anesthetized with Inactin (100 mg/kg, i.p., Byk Gulden Lomberg Chemische Fabrik GmbH, Konstanz, West Germany) and placed on a temperature-regulated micropuncture table and prepared for micropuncture as described previously (7). The left femoral artery was catheterized with a PE-50 polyethylene tube

to allow periodic blood sampling and estimation of mean femoral arterial pressure ($\overline{AP}$). $\overline{AP}$ was monitored with an electronic transducer (model P23Db, Statham Instruments Div., Gould Inc., Oxnard, Calif.) connected to a direct-writing recorder (model 7754A, Hewlett-Packard Co., Palo Alto, Calif). Polyethylene catheters were also inserted into the left and right jugular veins, and 7% inulin solution in 0.9% NaCl then was infused at a rate of 1.2 ml/h. Animals were divided into several groups, as described in detail below and summarized in Table I.

Study of glomerular dynamics. In 10 AICN (group 1A), 7 HICN (group 2), and 8 control rats (group 3), all of which were female, micropuncture measurements were carried out after a 30- to 45-min equilibration period as follows. Exactly timed (1- to 2-min) samples of fluid were collected from surface late proximal convolutions from each of 2–5 nephrons for determination of flow rate and inulin concentration and for calculation of single nephron glomerular filtration (SNGFR) and absolute proximal reabsorption (APR) rates. For this purpose, late surface convolutions of proximal tubules were located by observing the passage of lissamine green dye, which was injected rapidly (0.05 ml of a 5% solution) into the right jugular vein catheter. Inulin concentrations in tubule fluid were measured in duplicate using the method of Vurek and Pegram (8). Coincident with tubule fluid collections, two or three samples of femoral arterial blood were obtained in each period for determination of hematocrit and plasma concentrations of protein and inulin. In addition, two or three samples of urine from the experimental kidney were collected for determination of flow rate and inulin concentration and for calculation of total kidney inulin clearance. For these urine collections, indwelling ureteral polyethylene catheters (PE-10) were used. Inulin concentrations in plasma and urine were assayed with the macroanthrone method of Führ et al. (9). Time-averaged pressures were measured in surface glomerular capillaries ($\bar{P}_{GC}$), proximal tubules (P_T), and efferent arterioles (P_E) using a continuously recording, servo-null micropipette transducer system (model 3, Instrumentation for Physiology and Medicine, San Diego, Calif.) For these pressure measurements, micropipettes with outer tip diameters of 1–2 μm and containing 2.0 M NaCl were used. Hydraulic output from the servosystem was coupled electronically to a second channel of the Hewlett-Packard recorder by a pressure transducer.

To estimate the colloid osmotic pressure of plasma entering and leaving glomerular capillaries, protein concentrations (C) in femoral arterial (C_A) and surface efferent arteriolar (C_E) blood plasmas were measured, using the method of Viets et al. (10). From measurements of C_A and C_E, values for afferent (Π_A) and efferent (Π_E) arteriolar oncotic pressures could be calculated (11). These estimates of preglomerular and postglomerular plasma protein concentration and oncotic pressure permit calculation of single nephron filtration fraction (SNFF), initial glomerular plasma flow rate (Q_A), and glomerular capillary ultrafiltration coefficient (K_f), as well as resistances of single afferent (R_A) and efferent (R_E) arterioles, using equations described in detail elsewhere (11).

As discussed below, our initial experiments in AICN rats disclosed that SNGFR values were remarkably heterogeneous within a single kidney. To explore the mechanisms responsible for this high degree of intrarenal heterogeneity of SNGFR values, we obtained SNGFR and C_E values for the same nephron unit in five group 1A rats. This provided a means for defining the extent of variation in Q_A from glomerulus to glomerulus in a given kidney. For this purpose, the efferent arteriole and a proximal tubule segment belonging to the same glomerulus were identified by the topographical method of Briggs and Wright (12). Moreover, using two other similarly prepared AICN rats (group 1B), we determined SNGFR and glomerular capillary and proximal tubule hydraulic pressures, all for the same nephron units. 9 such units were studied in the kidney of one rat and

TABLE I
Summary of Experimental Groups of Rats

Group 1 AICN (n = 18)	A (n = 10):	measurements of SNGFR, APR, and the various determinants of SNGFR. Determination of SNGFR, Q_A, and K_f for the same nephron unit (n = 5).
	B (n = 2):	measurements of $\bar{P}_{GC}$, P_T, and SNGFR for the same nephron unit.
	C (n = 2):	measurements of peritubular capillary dynamics for each nephron unit.
	D (n = 4):	microinjection study to evaluate the possibility of inulin backleak in superficial nephrons.
Group 2 HICN (n = 7)		measurements of SNGFR and its determinants in each rat.
Group 3 Control (n = 8)		measurements of SNGFR and its determinants in each rat.

Kidneys from five rats of group 1A, two from group 1B, two from group 1C, seven from group 2, and three from group 3 were subjected to light, electron, and immunofluorescence microscopy.

10 in the other. 30 min before these measurements and collections, proximal tubules associated with specific surface glomeruli were identified in these two rats by observing the passage of ~5 nl of 0.1% lissamine green injected via sharpened glass pipettes (outer tip diameters of ~1 μm) into Bowman's space.

Study of proximal fluid reabsorption and peritubular capillary dynamics. As discussed in Results, an impressive correlation was obtained between SNGFR and APR values in the same nephron unit, despite wide variations in both of these quantities in a given AICN kidney. To explore the mechanism(s) responsible for this preservation of nearly perfect glomerulotubular balance in AICN, the forces governing peritubular capillary uptake of APR were determined for each single nephron unit in two AICN rats (group 1C) by the approach summarized below. After identification of the efferent arteriole and a proximal tubule segment belonging to a given glomerulus in these rats, APR, P_E, and the hydraulic pressure in distalmost surface branches of peritubular capillaries ($P_{C'}$) were determined for these nephron units. C_E was also determined, thus providing values for Q_A as well as initial peritubular capillary plasma flow rate (Q_E, where $Q_E = Q_A - SNGFR$), and initial peritubular capillary oncotic pressure. In addition, subcapsular space hydraulic pressure was measured in the vicinity of these units, and values obtained were taken to reflect interstitial hydraulic pressure (P_I).[1] Moreover, interstitial oncotic pressure (Π_I) was estimated from the value of protein concentration measured in the renal hilar lymph fluid. This fluid was obtained by inserting micropipettes (outer tip diameters of ~25 μm) into intact renal hilar lymph vessels (13).[2]

According to the Starling relationship, the rate of peritubular capillary uptake of APR is given by $APR = K_r \cdot \bar{P}_r = K_r (\Delta\Pi - \Delta P) = K_r \cdot [(\bar{\Pi}_C - \Pi_I) - (\bar{P}_C - P_I)]$, where K_r and $\bar{P}_r$ represent peritubular capillary reabsorption coefficient and mean net reabsorptive pressure, respectively; $\Delta\Pi$ and ΔP are the mean peritubular transcapillary oncotic and hydraulic pressure differences; $\bar{\Pi}_C$ and $\bar{P}_C$ are the mean peritubular intracapillary oncotic and hydraulic pressures; and Π_I and P_I are the corresponding pressures in the surrounding cortical interstitium. $\bar{P}_C$ was estimated from the expression $(P_E + P_{C'})/2$.[3] K_r and $\bar{P}_r$, and thus $\Delta\Pi$ and $\bar{\Pi}_C$, were calculated with a differential equation that gives the rate of decline of protein concentration with distance along an idealized peritubular capillary. This equation, together with its derivation and the method for its solution, is discussed in detail elsewhere (17, 18).

Microinjection studies

Microinjections with tritiated [^{3}H]inulin were performed in a separate group of four female AICN rats (group ID). These studies were carried out to assess the reliability of inulin as a marker for superficial SNGFR in AICN. In these experiments, modest diuresis was induced by a continuous infusion of 5% mannitol in 0.9% NaCl at a rate of 6 ml/h to permit rapid, serial urine collections. Known volumes (3–10 nl) of lissamine green-stained [^{3}H]inulin in isotonic saline were injected into early proximal tubules of the left kidney, in 30–90 s, with sharpened glass micropipettes with outer tip diameters of ~5 μm. With a calibrated transfer pipette, known volumes of isotope were transferred to (*a*) microinjection pipettes and (*b*) pipettes that were used for standardization of activity of the injectate. The experimental protocol, assay procedure, and calculation of percent recovery in these nephrons are described in detail elsewhere (19).

Light, electron, and immunofluorescence microscopy

The kidneys of rats subjected to micropuncture study (AICN—groups 1A, 1B, and 1C; HICN—group 2 and control group 3) were prepared for light, electron, and immunofluorescence microscope examination. After micropuncture measurements, a midcoronal section of each kidney was snap-frozen in isopentane prechilled in liquid nitrogen and processed for immunofluorescence microscopy as described previously (20). An adjacent section of tissue was fixed in 10% buffered formalin for microscopy. In addition, thin sections of cortex from these kidneys were fixed in modified Karnovsky's fixative (1.5% formaldehyde, 2% gluteraldehyde in 0.1 M Na_2HPO_4 buffer, pH 7.4) and processed for electron microscopy as described previously (21). Tissue sections for immunofluorescence microscopy were stained with fluorescein-conjugated monospecific rabbit antiserum to rat IgG, C3, albumin, and fibrinogen prepared in our laboratories (20) and with fluorescein-conjugated monospecific rabbit antisera to sheep IgG absorbed with rat IgG conjugated to Sepharose 4B (Pharmacia Fine Chemicals, Div. of Pharmacia Inc., Piscataway, N. J.) before use. The antiserum to rat IgG was absorbed with sheep IgG before staining of sections from HICN rats. Immunofluorescence sections were also stained with anti-Fx1A antiserum.

RESULTS

General results

Table II summarizes the results of whole animal data obtained from groups 1A, 2, and 3. The three groups were similar with respect to body weight, whereas average values for kidney weight in AICN and HICN rats were significantly higher than in the control group. Values for systemic blood hematocrit (Hct) in femoral artery were similar among groups, although average values tended to be slightly lower in AICN rats than in the others. 24-h urinary albumin excretion rates ($U_{alb}V$) averaged 3±0 mg in control animals, compared

[1] Although the subcapsular space in normal hydropenic rats is not wide enough to allow meaningful assessment of P_I, pipettes were easily inserted into this space in AICN rats, presumably reflecting the interstitial edema known to be present in AICN kidneys. Values for subcapsular pressure thus measured were quite uniform from area to area (range, 1.0–2.5 mm Hg).

[2] Because renal lymph is thought to originate primarily in the cortex (14–16), Π_I was estimated from the value of protein concentration measured in this lymph fluid. Although Π_I values could conceivably differ from region to region in the cortex, the low absolute values obtained (2.5 mm Hg for both rats) indicate that Π_I contributes little to the overall net peritubular capillary reabsorptive force.

[3] Although the true profile of P_C with distance along peritubular capillaries may not be strictly linear, this assumption is a reasonable approximation in view of our finding that values of P_C measured at second-order branches of efferent arterioles are roughly midway between measured values for P_E and $P_{C'}$.

TABLE II
Whole-Animal Data from AICN, HICN, and Control Rats

	BW	KW	Hct	$U_{alb}V$	C_A	$\overline{AP}$	C_{IN}
	g		*vol%*	*mg/d*	*g/dl*	*mm Hg*	*ml/min*
AICN (group 1A) (n = 10)	217±6	1.14±0.06	46.7±0.3	182±32	5.4±0.2	116±1	0.58±0.02
P*	NS	<0.001	<0.0025	<0.001	NS	NS	<0.001
HICN (group 2) (n = 7)	210±4	1.09±0.08	51.6±1.2	112±16	5.5±0.2	117±4	0.64±0.04
P*	NS	<0.01	NS	<0.001	NS	NS	<0.05
Control (group 3) (n = 8)	221±6	0.82±0.02	49.6±0.6	3±0	5.4±0.1	117±3	0.81±0.05

BW, body weight; KW, kidney weight.
Values are expressed as mean±1 SE.
* Calculated from unpaired data vs. control; NS, $P > 0.05$.

with much higher values in AICN and HICN rats, which averaged 182±32 mg/d (range, 92–275) in AICN and 112±16 (range, 37–143) in HICN. Nevertheless, values for systemic plasma protein concentration, C_A, in both AICN and HICN rats remained at control levels. Average values for $\overline{AP}$ are also shown in Table II and did not differ among the three groups studied. Finally, whereas values for total kidney inulin clearance averaged 0.81±0.05 ml/min in control rats, a value typical for this strain of rats measured previously by us (7) and others (22) under normal hydropenic conditions, significantly lower mean values were noted in AICN and HICN groups.

Micropuncture studies

Glomerular dynamics in rats with HICN. As with whole kidney inulin clearance, mean values for SNGFR were some 30% lower and values for Q_A were ~25% lower in HICN rats than in controls (Table III). The mean value for SNFF in HICN was therefore slightly but not significantly lower than in controls. Proximal tubule hydraulic pressures, P_T, were only slightly but significantly higher in HICN than in control rats, whereas $\overline{P}_{GC}$ values were substantially higher in the former, on average by 10 mm Hg, so that the mean value for ΔP was also significantly higher in HICN than in controls. As also shown in Table III, mean values for Π_A and Π_E did not differ significantly between control and HICN animals. Thus, whereas the mean value for Π_E essentially equalled ΔP in controls, Π_E was uniformly lower than ΔP in HICN rats, denoting filtration pressure disequilibrium in HICN but not in control rats. Unique values for K_f could therefore be calculated in HICN but not in control rats.[4]

[4] In the HICN group, values for $\Pi_E/\overline{\Delta P}$ ranged from 0.69 to 0.94, whereas in all but one rat from control, $\Pi_E/\Delta P$ values were >0.95. Only minimum values for K_f could therefore be calculated for the controls, and the average is given in Table III.

The mean of the unique values for K_f obtained in the HICN group averaged 0.026±0.002 nl/(s·mm Hg), a value more than 50% lower than the mean *minimum* K_f value calculated in controls (0.067±0.007). In HICN rats, R_E and R_A averaged 4.0±0.5 and 4.2±0.7 × 10^{10} dyn·s·cm^{-5}, respectively. While the average value for R_A was not statistically different from that of control rats, the average R_E value was significantly higher (by ~70%). Therefore, despite the higher average value for $\overline{P}_{GC}$ resulting from this marked rise in R_E in HICN rats, SNGFR fell significantly, due primarily to the measured decline in K_f.

Glomerular dynamics in rats with AICN. In AICN, the average value for whole-kidney inulin clearance was ~30% lower than that in control rats (Table II), whereas the average SNGFR value measured in superficial proximal tubules remained at a level only slightly but not significantly below that of controls (Table III). Since, as discussed below, SNGFR values differ markedly from nephron to nephron in AICN kidneys, it is conceivable that the calculated average SNGFR value based on the collections from a few nephrons per kidney may not be truly representative of the whole population.

In contrast to the overall functional similarity between HICN and AICN when analyzed in terms of average values obtained from kidney to kidney, marked differences between AICN and HICN were noted when evaluated from nephron to nephron in a given kidney. Thus, as shown in Fig. 1, the depression in SNGFR values in HICN rats proved to be a uniform and homogeneous response within a given kidney, the extent of variation in SNGFR values per kidney not being different from that in normal rats (23). By contrast, marked variability in SNGFR values from nephron to nephron was noted in each kidney of AICN rats, a finding similar to that of Allison et al. (5).

To explore the mechanisms responsible for this marked functional heterogeneity in AICN animals, two additional AICN rats (group 1B) having albumin-

TABLE III
Summary of Single Nephron Function in AICN, HICN, and Control Rats

	SNGFR	$\bar{P}_{GC}$	P_T	$\overline{\Delta P}$	Π_A	Π_E	$\Pi_E/\overline{\Delta P}$	SNFF	Q_A	R_A	R_E	K_f
	nl/min			*mm Hg*					*nl/min*	*×10¹⁰ dyn·s·cm⁻⁵*		*nl/(s·mm Hg)*
AICN (group 1A) (n = 10)	25.8±2.9	57.6±0.9	14.9±0.6	42.6±0.8	17.3±0.4	35.3±1.4	0.83±0.04	0.36±0.01	73±9	4.0±0.5	4.2±0.6	0.030±0.005[5]
P*	NS	<0.001	<0.01	<0.001	NS	NS	<0.001	NS	NS	NS	<0.01	<0.001
HICN (group 2) (n = 7)	21.6±2.0	57.4±0.9	14.7±0.6	42.7±1.0	18.0±0.7	35.3±1.3	0.83±0.03	0.36±0.02	61±7	4.2±0.7	4.0±0.5	0.026±0.002
P*	<0.05	<0.001	<0.01	<0.001	NS	NS	<0.001	NS	NS	NS	<0.025	<0.001
Control (group 3) (n = 8)	29.9±2.4	47.4±0.4	12.4±0.4	35.0±0.5	17.4±0.5	37.1±0.8	1.05±0.02	0.39±0.01	80±7	3.7±0.3	2.5±0.2	≥0.067±0.007

Values are expressed as mean±1 SE.

* Calculated from unpaired data vs. control; NS represents $P > 0.05$.

[5] In eight rats in the AICN group, $\Pi_E/\overline{\Delta P}$ values ranged from 0.69 to 0.94. Unique values for K_f were therefore determined in these animals and averaged 0.026±0.005 nl/(s·mm Hg). In the remaining rat, $\Pi_E/\overline{\Delta P}$ was 1.05, yielding a minimum K_f value of 0.061 nl/(s·mm Hg). For all nine rats, the average K_f value of 0.030±0.005 was significantly less than that of the control group.

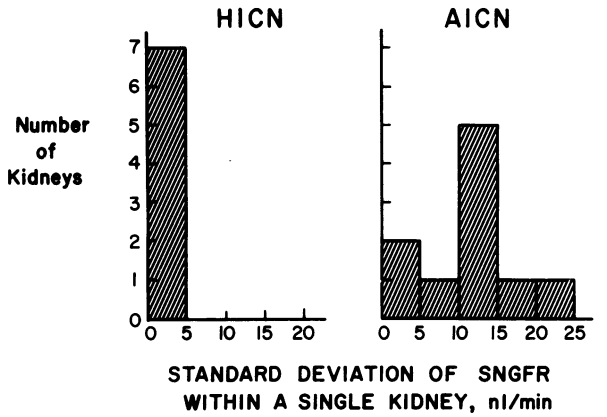

FIGURE 1 Frequency histogram depicting the range of standard deviation in SNGFR values calculated for each of 7 HICN (group 2) and 10 AICN (group 1A) animals.

uria similar in magnitude to that of group 1A rats were subjected to micropuncture study. Because these rats each possessed nine or more surface glomeruli accessible to direct micropuncture study, we determined paired values for $\overline{P}_{GC}$ and P_T in the same nephron unit. As shown on the abscissa of Fig. 2A, values for P_T varied markedly from nephron to nephron in these two AICN kidneys (range, 8–31 mm Hg). Individual values for $\overline{P}_{GC}$ also varied markedly (range, 45–74 mm Hg). As can be seen, however, nephrons with high values for P_T were regularly associated with high values for $\overline{P}_{GC}$, and vice versa. Accordingly, ΔP values calculated from these paired measurements of $\overline{P}_{GC}$ and P_T remained relatively constant from glomerulus to glomerulus (Fig. 2B). As shown in Fig. 2B, values for SNGFR varied markedly from nephron to nephron, despite these nearly uniform ΔP values, indicating that the wide variation in SNGFR observed in AICN was not due primarily to equivalent variation in ΔP. Likewise, since the oncotic pressure of the plasma entering all glomeruli must be the same within a given kidney, this determinant can also be excluded as a cause of the marked nephron-to-nephron heterogeneity in SNGFR values in AICN.

In five rats in group 1A, we also obtained paired values for SNGFR and Q_A for a given glomerulus to evaluate the contribution of Q_A to the observed marked heterogeneity in filtration rates seen in AICN rats. Fig. 2C presents the paired data obtained in 21 nephrons from these five AICN animals. As shown, wide variation in SNGFR was again noted and was associated with similarly marked variation in paired values for Q_A. Of importance, a strong correlation was detected between these paired measures such that when Q_A was low, SNGFR was also low and vice versa ($r = 0.71$, $P < 0.001$). Finally, K_f, the only remaining determinant of SNGFR, was estimated for individual glomeruli from values of Π_A, $\overline{\Delta P}$,[6] SNGFR, and Q_A. As can be seen in Fig. 2D, values for K_f varied markedly from glomerulus to glomerulus and, as with Q_A, correlated closely with SNGFR values measured in these same glomeruli ($r = 0.87$, $P < 0.001$).

APR and peritubular capillary dynamics in AICN. In addition to evaluation of SNGFR and its individual determinants in AICN rats, measurements of APR were also obtained in individual surface nephrons, and the resulting values were examined in relation to SNGFR values for these same nephrons (group 1A). As shown in Fig. 3, APR values varied markedly from nephron to nephron in a given AICN kidney. Of importance, however, a highly significant correlation was found between SNGFR and APR values for a given nephron ($r = 0.87$, $P < 0.001$). Similar marked variation in absolute values for SNGFR and APR was detected in two AICN rats (group 1C), in which many paired measurements of SNGFR and APR were obtained for the same nephron unit in each kidney. Thus, as shown in Fig. 4A, despite the typically marked nephron-to-nephron heterogeneity of SNGFR values seen in each AICN kidney, nearly perfect glomerulotubular balance was achieved. As a result, tubule fluid/plasma inulin concentration ratios, a measure of end-proximal fractional sodium reabsorption, were remarkably similar from one nephron to another (Fig. 4B).

To define the mechanisms responsible for this close correlation between SNGFR and APR, we measured the various determinants of peritubular capillary uptake of APR in individual nephron units. The values for these individual uptake forces, namely, Q_E, P_E, and Π_E, measured at the distal end of surface efferent arterioles (i.e., the inlet to the peritubular capillary network) are given in Fig. 5A–C, together with paired SNGFR values determined for the same nephron units. Thus, as shown in Fig. 5A, whereas values for Q_E varied widely, ranging from 48 to 162 nl/min, we failed to detect any significant correlation between individual values for Q_E and paired measurements of APR. Likewise, although hydraulic pressure at the peritubular capillary inlet, P_E, was found to vary only slightly from network to network (16–20 mm Hg), no significant correlation with APR could be demonstrated, as shown in Fig. 5B. By contrast, values for initial peritubular capillary plasma protein concentration, C_E, and hence oncotic pressure, Π_E, which varied widely (range, 23–42 mm Hg), correlated closely with paired

[6] Because $\overline{\Delta P}$ values were remarkably constant from glomerulus to glomerulus in a single kidney, the average ΔP value for each kidney was employed for this computation.

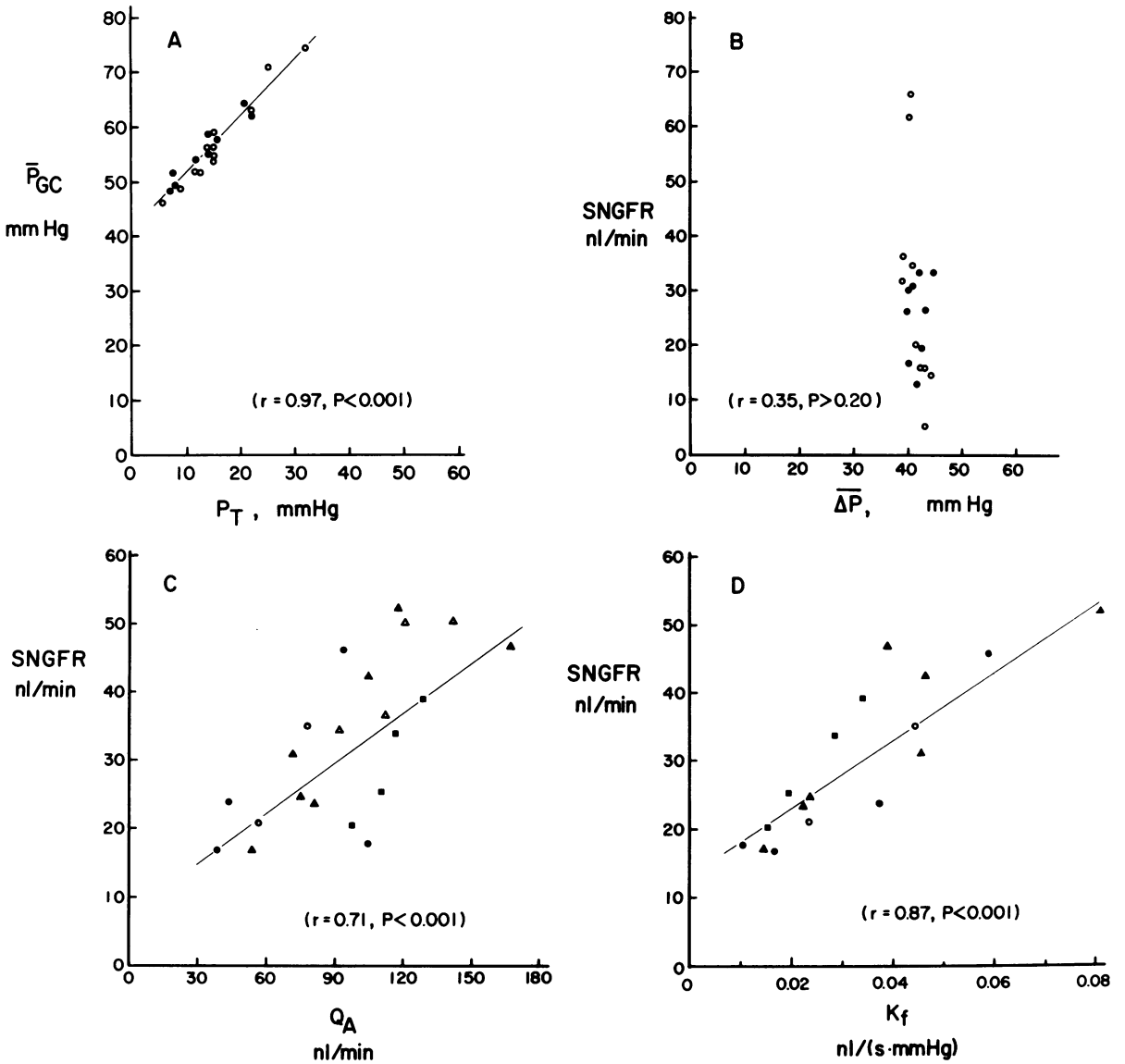

FIGURE 2 (A and B) Correlations between proximal tubule hydraulic pressure (P_T) and mean glomerular capillary hydraulic pressure ($\bar{P}_{GC}$) and between $\Delta\bar{P}$ and SNGFR measured in the same nephrons from two AICN (group 1B) rats. (C and D). Correlations between glomerular plasma flow rate (Q_A) and SNGFR and between K_f and SNGFR determined in the same nephrons from five AICN (group 1A) animals. Data obtained from a single kidney are identified by like symbol.

APR values, as shown in Fig. 5C.[7] In view of this important contribution of peritubular capillary oncotic pressure to the observed value of APR, it is hardly surprising that APR also varied closely with $\bar{P}_r$, as shown in Fig. 5D. Finally, K_r, the last remaining determinant of peritubular capillary uptake of APR, was calculated from individual values of Q_E, Π_E, P_E, P_{C^1}, P_I, and APR estimated for the same proximal tubule-peritubular capillary unit. Thus, in addition to $\bar{P}_r$, which influenced APR so strongly, it is apparent from Fig. 5E that APR also varied closely with K_r.

[7] We also calculated the slope of the linear regression line for the relationship between Π_E and APR in each of the seven rats (the group shown in Fig. 3). The calculated slopes were significantly greater than zero, averaging 1.19±0.31 ($P < 0.01$), a value similar to that found in group 1C (Fig. 5C).

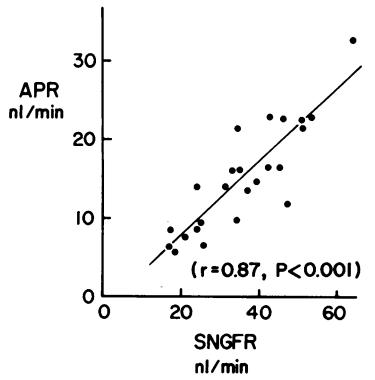

FIGURE 3 Correlation between SNGFR and APR measured in 24 nephrons from 7 AICN (group 1A) rats.

Microinjection studies

The measured wide variation in SNGFR and APR within a given AICN kidney could be due to a variable transtubular inulin leak. To evaluate this possibility, we determined the ipsilateral kidney recovery rate of [^{3}H]inulin microinjected into surface proximal tubules in 13 nephrons from four AICN rats (group 1D) having albuminuria equivalent to that measured in group 1A. Recovery rates uniformly were >90% and averaged 95.6±0.7%, arguing against the presence of a significant degree of inulin leakage in surface nephrons in AICN.

Light, electron, and immunofluorescence microscopy

Light microscopy. A diffuse, mild thickening in glomerular basement membranes (GBM) was detected in all AICN kidneys, whereas glomeruli of HICN were optically normal. Structural changes in the tubules were absent in HICN, whereas focal tubule dilatation, involving <10% of proximal tubules, was present in most AICN kidneys. These tubule changes tended to be focal and generally milder than those described previously by Allison et al. (5) and Mendrick et al. (4), in all likelihood reflecting greater chronicity and/or severity of their models. Similarly, interstitial changes were infrequent and mild in the present study, in contrast to more pronounced interstitial abnormalities found in the studies of others (4, 5).

Electron microscopy. Subepithelial electron-dense deposits were distributed uniformly along peripheral capillary loops and mesangial reflections of the GBM in HICN rats. Despite these deposits, the underlying GBM (lamina densa and lamina rara interna) had a normal appearance (Fig. 6A). Fusion of epithelial foot processes was prominent in all glomeruli. Immune deposits in AICN rats tended to be less electron dense than those of HICN rats and their distribution was less uniform. Thus, in some areas the GBM appeared thickened, whereas it was of normal thickness in areas without deposits (Fig. 6B). Blunting and fusion of epithelial foot processes were directly related to the presence of the electron-dense deposits and the GBM abnormalities, showing considerable variation in degree from one glomerulus to another (Fig. 6C and D) and from one loop to another within the same glomerulus (Fig. 6B).

Immunofluorescence microscopy. Finely granular deposits of sheep IgG were evenly distributed along the capillary walls of all glomeruli in each HICN kidney studied. Less intensely staining deposits of rat IgG and C3 were present in an identical distribution along capillary walls. In AICN kidneys, deposits of rat IgG and Fx1A showed considerably greater variation in distribution within and among glomeruli. Moreover, the C3 deposits in AICN were either absent or much less intense than those in HICN. By contrast, reabsorption droplets containing plasma proteins were present within glomerular epithelial cells in almost all kidneys from rats with AICN, whereas these droplets were nearly absent in HICN kidneys. In AICN kidneys, considerable variation among glomeruli was also found in this regard; a small number of glomeruli ex-

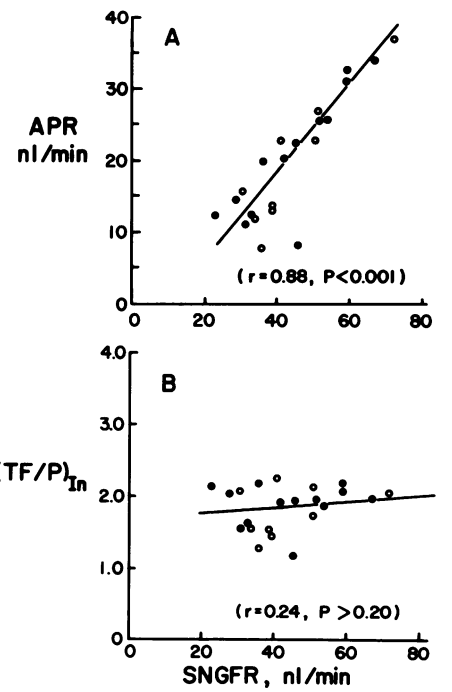

FIGURE 4 Correlation between SNGFR and APR (A) and between SNGFR and $(TF/P)_{In}$ (B) obtained from two AICN (group 1C) rats. Like symbols identify data from a single rat.

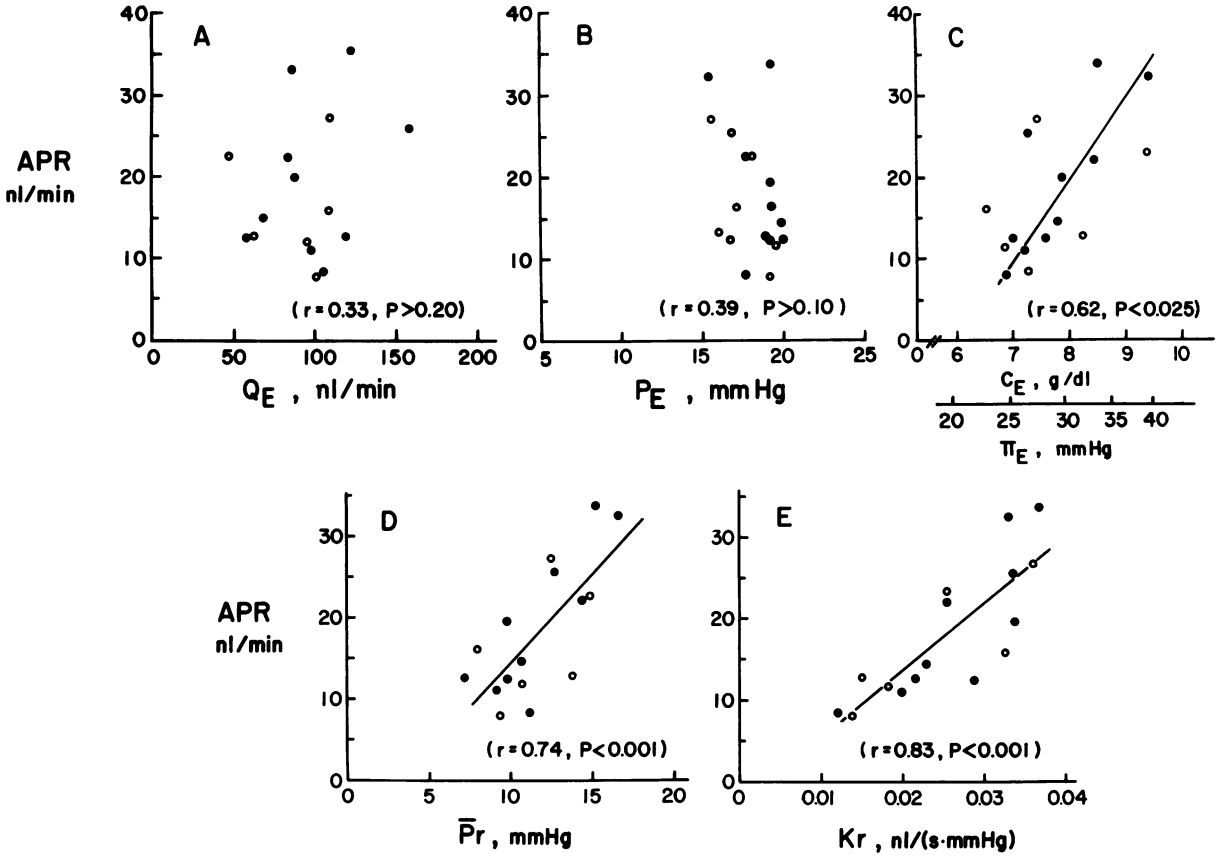

FIGURE 5 Correlations between APR and adjacent efferent arteriolar plasma flow rate (Q_E) (A); adjacent efferent arteriolar hydraulic pressure (P_E) (B); adjacent efferent arteriolar plasma protein concentration (C_E) or oncotic pressure (Π_E) (C); adjacent mean net peritubular capillary reabsorptive pressure ($\bar{P}_r$) (D); and adjacent peritubular capillary reabsorption coefficient (K_r) (E) in two AICN (group 1C) rats. Like symbols identify data from a single rat.

hibited many droplets, whereas many other glomeruli lacked any traces of epithelial droplets. Frequently, all of the droplets in a glomerulus were present within a single lobule.

Some difference between these two models were also found in tubules: focal deposits of IgG along the brush border were present in a small number (always <10%) of proximal tubules in each section from AICN but were not found in HICN kidneys. By contrast, albumin reabsorption droplets were much less frequently observed in the tubules of AICN than in those of HICN. Instead, the major feature demonstrated by immunofluorescence in AICN kidneys was the presence of large casts containing plasma proteins in a small number of dilated tubules. The casts frequently showed diffuse intense staining for albumin, and to a lesser extent, also contained C3, IgG, and fibrinogen. Such plasma protein casts were nearly always absent in HICN kidneys. Brush border staining for Fx1A showed a normal pattern in all HICN kidneys and in the majority of proximal tubules in each AICN kidney studied. In <10% of proximal tubules of AICN kidneys, this Fx1A staining was decreased or entirely absent.

DISCUSSION

As has been demonstrated (1–5), injection of an antigen derived from the brush borders of proximal tubule epithelial cells (AICN), or heterologous antibody raised to this antigen (HICN), induces subepithelial deposits of immunoglobulin and host complement and an overall glomerular lesion morphologically indistinguishable from membranous glomerulopathy in man. Although the time-course required to establish these two models differs considerably, i.e., 2 wk in HICN and several months in AICN, we found many qualitative

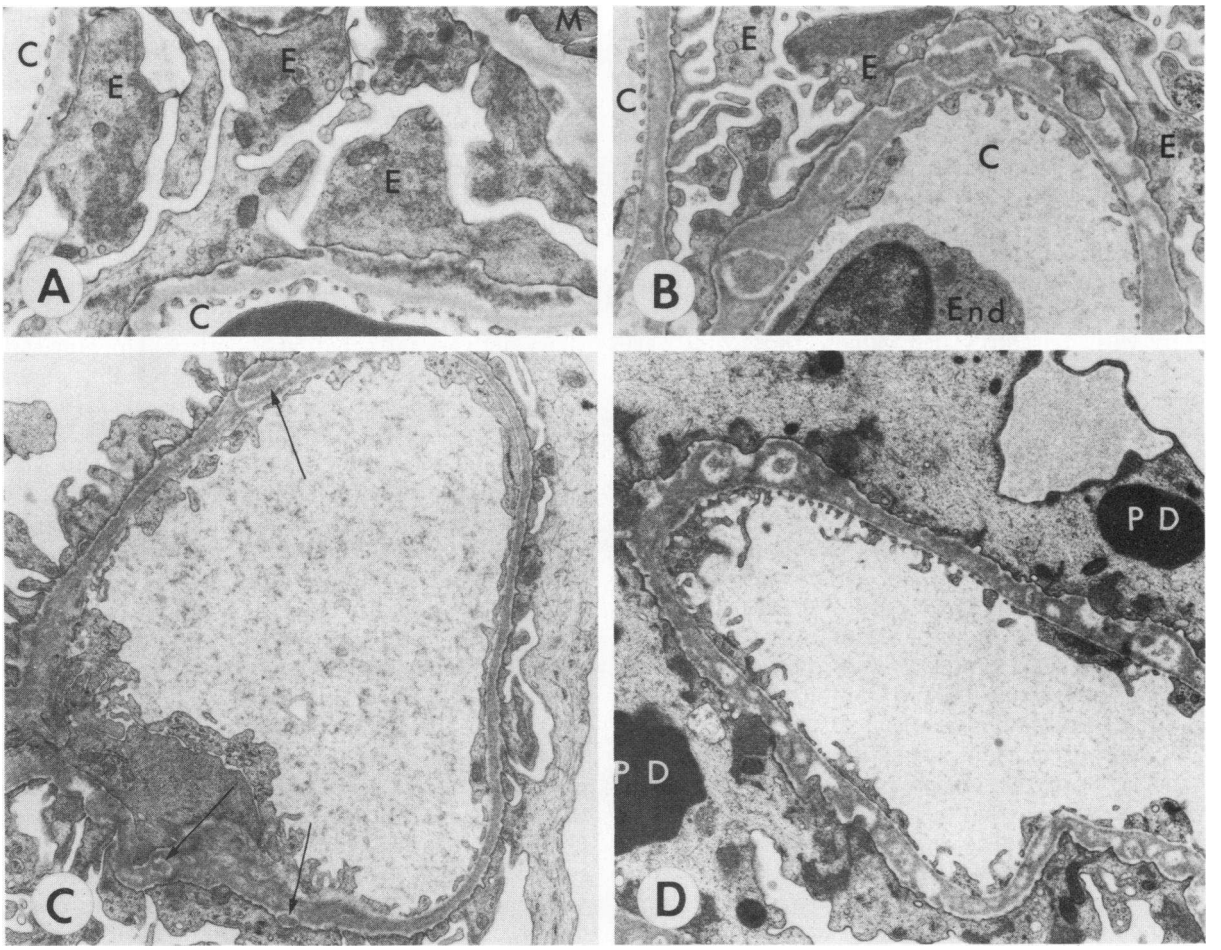

FIGURE 6 Electron micrographs of glomerular capillary loops from (A) a rat with HICN, showing confluent subepithelial electron-dense deposits, effacement of epithelial foot processes and a normal-appearing GBM; (B) a rat with AICN, showing several discrete electron-dense deposits surrounded by a clear space in the thickened GBM. One capillary loop (left side of the figure) exhibits fewer deposits and a GBM of normal thickness covered by normal slender foot processes; (C) a rat with AICN, showing smaller electron-dense deposits (arrows) and minimal GBM changes; (D) the rat shown in C (another glomerulus), showing a "moth-eaten" GBM and extensive effacement of glomerular epithelial foot processes. The epithelium also contains several large protein reabsorption droplets. Capillary lumen (C); epithelium (E); endothelial cell (*End*); mesangial cell (*M*); protein reabsorption droplets (*PD*). A and B, ×12,000. C and D, ×8,000.

similarities between them. AICN and HICN both gave rise to impressive albuminuria and mild to moderate reduction in SNGFR, and both forms of glomerulopathy were associated with marked alterations in $\overline{P}_{GC}$, ΔP, R_E, and K_f.

An important functional difference between AICN and HICN is that, whereas uniform and homogeneous depression of SNGFR characterized HICN kidneys, markedly different SNGFR values were measured from nephron to nephron in the kidneys of AICN rats. Immunofluorescence microscopy carried out in each AICN kidney also revealed marked variation in the degree of glomerular deposits of immunoglobulin and C3. By contrast, such deposits were uniformly distributed from glomerulus to glomerulus in HICN. This diverse immunofluorescence pattern in AICN glomeruli is similar to that described by Allison et al. (5).

Allison and co-workers (5) also demonstrated that APR varied widely from nephron to nephron in AICN but that APR remained proportional to SNGFR, so that each nephron unit exhibited a high degree of glomerulotubular balance. A similar tight correlation be-

tween SNGFR and APR was also evident in the present study. Of the three determinants for SNGFR which could account for the observed nephron-to-nephron variability in AICN, namely, ΔP, Q_A, and K_f, ΔP was found not to be important, because values for ΔP were remarkably constant from glomerulus to glomerulus. By contrast, values for Q_A exhibited marked variability from glomerulus to glomerulus and also correlated closely with individually paired SNGFR values, such that when Q_A was low SNGFR was low and vice versa. Values for K_f also varied widely and again correlated closely with paired SNGFR values. Thus, wide variations in Q_A and K_f proved to underlie the marked heterogeneity in SNGFR values seen in AICN. Because K_f consists of two components, namely total glomerular capillary surface area and the effective capillary hydraulic permeability to water, wide variation in either or both of them could account for the observed variation in K_f. It is, therefore, conceivable that the tendency of K_f to vary in parallel with Q_A (although just short of statistical significance; $P > 0.10$) may reflect a single glomerular alteration, namely, variable occlusion of glomerular capillary loops, thereby bringing about concomitant reductions in filtering surface area as well as in perfused channels.

The impressive tight correlation observed between $\bar{P}_r$ and APR in the present study (Fig. 5D) points strongly to the possibility that the observed marked nephron-to-nephron variation in APR values is primarily a consequence of similar marked variation in the mean net reabsorptive force acting across the peritubular capillary network adjacent to the proximal tubule under study. Of the various forces determining the value of $\bar{P}_r$, inlet values of peritubular capillary plasma protein concentration (C_E), hence oncotic pressure (Π_E), appear to play the major roles. By contrast, the intracapillary hydraulic force measured at both the proximal and distal ends of the peritubular capillary network was not systematically different from one nephron unit to another (Fig. 5B). Moreover, although the initial peritubular capillary plasma flow rate, Q_E, the remaining potential determinant of the dispersion in $\bar{P}_r$ values, varied markedly in a given kidney (Fig. 5A), we failed to detect any significant correlation between this variable and paired values for APR. This is not surprising in view of the fact that the peritubular capillary bed normally operates at conditions far from pressure equilibrium (in contrast to the process of glomerular filtration). Thus, over the range of Q_E values measured in AICN rats, the impact of this quantity on the length-averaged value of Π_E and therefore $\bar{P}_r$ can be expected to be small (17). On the other hand, with more extreme reductions in Q_E, below ~50 nl/min, the change in Q_E per se will serve to lower $\bar{P}_r$ and therefore APR (17).

In addition to $\bar{P}_r$, APR also correlated closely with paired estimates of the peritubular capillary reabsorption coefficient, K_r, a variable that also ranged widely from nephron unit to nephron unit (Fig. 5E). As with K_f, K_r is best expressed in terms of its two components, peritubular capillary surface area and the effective capillary hydraulic permeability. Marked heterogeneity in either or both of these terms could account for the observed wide variation in K_r. Values for K_r varied from nephron to nephron in direct proportion to the value of Q_E entering the same peritubular capillary network (although just short of achieving statistical significance, $P > 0.10$), suggesting that changes in surface area were responsible for parallel alterations both in Q_E and K_r, not unlike the circumstance described above for the glomerulus (i.e., Q_A and K_f).

On the basis of observed correlations, we suggest the following mechanism to account for the parallel changes in SNGFR and APR noted among individual surface nephron units in circumstances of heterogeneous glomerular function such as AICN. The open circle in Fig. 7 depicts typical values for SNGFR and APR in normal hydropenic rats. The ratio between APR and SNGFR defines the base level of fractional proximal reabsorption, so that any point on the dashed straight line in Fig. 7 indicates maintenance of perfect glomerulotubular balance. We have already shown that variations in K_f and glomerular plasma flow rate, Q_A, account for the wide range of SNGFR values observed in AICN. Thus, when values for K_f and Q_A in a given glomerulus are reduced, SNGFR is also reduced, as indicated by the leftward direction of the solid arrow. The reduction in K_f also dictates a concurrent fall in postglomerular plasma protein concentration, C_E, hence a decline in Π_E. Such a correlation between K_f and Π_E was indeed demonstrated in group 1A experimental animals ($P < 0.001$). We suggest that the fall in Π_E brings about the reduction in $\bar{P}_r$ and thereby the decrease in APR also, as shown by the

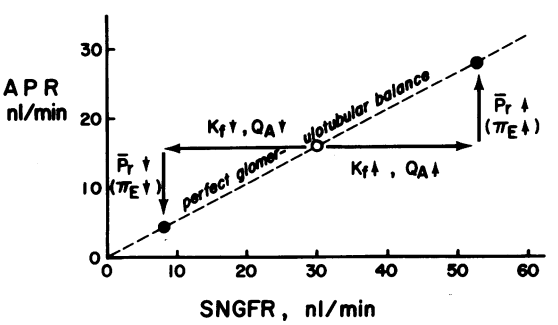

FIGURE 7 Schematic presentation of the proposed mechanism of glomerulotubular balance operating in each nephron unit of AICN kidneys.

downward arrow in Fig. 7. As also shown, increases in K_f in association with increased Q_A lead not only to increased values for SNGFR but also to concurrent increases in C_E, and, in turn, in $\overline{P}_r$ and APR, accounting for the glomerulotubular balance also observed in such hyperfunctioning nephron units. Thus, irrespective of whether AICN leads to hypofiltration or hyperfiltration, it is possible that the extent of glomerular damage or lack thereof dictates the microvascular conditions downstream to the glomerulus and, in so doing, establishes the conditions that eventuate in nearly perfect glomerulotubular balance.[8] Clearly, the mechanism proposed by no means rules out the operation of luminal or epithelial factors that might also contribute to the overall regulation of proximal fluid reabsorption in AICN (24).

ACKNOWLEDGMENTS

The authors are grateful to Ms. Denise Voss for her expert secretarial assistance.

These studies were supported largely by grants from the U. S. Public Health Service (AM-19467 and AM-27122) and by Veterans Administration research funds.

REFERENCES

1. Edgington, T. S., R. J. Glassock, and F. J. Dixon. 1967. Autologous immune complex pathogenesis of experimental allergic glomerulonephritis. *Science (Wash. D. C.).* **155:** 1432–1434.
2. Couser, W. G., M. M. Stilmant, and C. Darby. 1976. Autologous immune complex nephropathy. I. Sequential study of immune complex deposition, ultrastructural changes, proteinuria and alterations in glomerular sialoprotein. *Lab. Invest.* **34:** 23–30.
3. Salant, D. J., D. Christine, and W. G. Couser. 1980. Experimental membranous glomerulonephritis in rats. *J. Clin. Invest.* **66:** 71–81.
4. Mendrick, D. L., B. Noble, J. R. Brentjens, and G. A. Andres. 1980. Antibody-mediated injury to proximal tubules in Heymann nephritis. *Kidney Int.* **18:** 328–343.
5. Allison, M. E. M., C. B. Wilson, and C. W. Gottschalk. 1974. Pathophysiology of experimental glomerulonephritis in rats. *J. Clin. Invest.* **53:** 1402–1423.
6. Mancini, C., A. O. Carbonara, and J. R. Heremans. 1965. Immunochemical quantitation of antigens by single radial immunodiffusion. *Immunochemistry.* **2:** 235–254.
7. Maddox, D. A., C. M. Bennett, W. M. Denn, R. J. Glassock, D. Knutson, T. M. Daugharty, and B. M. Brenner. 1975. Determinants of glomerular filtration in experimental glomerulonephritis in the rat. *J. Clin. Invest.* **55:** 305–318.
8. Vurek, G. G., and S. E. Pegram. 1966. Fluorometric method for the determination of nanogram quantities of inulin. *Anal. Biochem.* **16:** 409–419.
9. Führ, J., J. Kazmarczyk, and C. D. Krüttgen. 1955. Eine einfache colorimetrische Methode zur Inulinbestimmung für Nierenclearanceuntersuchungen bei Stoffwechselgesunden und Diabetikern. *Klin. Wochenschr.* **33:** 729–730.
10. Viets, J. W., W. M. Deen, J. L. Troy, and B. M. Brenner. 1978. Determination of serum protein concentration in nanoliter blood samples using fluorescamine or *o*-phthalaldehyde. *Anal. Biochem.* **88:** 513–521.
11. Deen, W. M., C. R. Robertson, and B. M. Brenner. 1972. A model of glomerular ultrafiltration in the rat. *Am. J. Physiol.* **223:** 1178–1183.
12. Briggs, J. P., and F. S. Wright. 1979. Feedback control of glomerular filtration rate: site of the effector mechanism. *Am. J. Physiol.* **236:** F40–F47.
13. Ichikawa, I., and B. M. Brenner. 1979. Mechanism of inhibition of proximal tubule fluid reabsorption following exposure of the kidney to the physical effects of expansion of extracellular fluid volume. *J. Clin. Invest.* **64:** 1466–1474.
14. Bell, R. D., W. L. Parry, and W. G. Grundy. 1973. Renal lymph sodium and potassium concentrations following renal vasodilation. *Proc. Soc. Exp. Biol. Med.* **143:** 499–501.
15. Wolgast, M., E. Persson, J. Schnermann, H. Ulfendahl, and P. Wunderlich. 1973. Colloid osmotic pressure of the subcapsular interstitial fluid of rat kidneys during hydropenia and volume expansion. *Pfluegers Arch. Eur. J. Physiol.* **340:** 123–131.
16. O'Morchoe, C. C. C., P. J. O'Morchoe, and E. J. Donati. 1975. Comparison of hilar and capsular renal lymph. *Am. J. Physiol.* **229:** 416–421.
17. Deen, W. M., C. R. Robertson, and B. M. Brenner. 1973. A model of peritubular capillary control of isotonic fluid reabsorption by the renal proximal tubule. *Biophys. J.* **13:** 340–365.
18. Blantz, R. C., and B. J. Tucker. 1975. Determinants of peritubular capillary fluid uptake in hydropenia and saline and plasma expansion. *Am. J. Physiol.* **228:** 1927–1935.
19. Baylis, C., H. R. Rennke, and B. M. Brenner. 1977. Mechanisms of the defect in glomerular ultrafiltration associated with gentamicin administration. *Kidney Int.* **12:** 344–353.
20. Hoyer, J. R. 1980. Tubulointerstitial immune complex nephritis in rats immunized with Tamm-Horsfall protein. *Kidney Int.* **17:** 284–292.
21. Seiler, M. W., H. G. Rennke, M. A. Venkatachalam, and R. S. Cotran. 1977. Pathogenesis of polycation-induced alterations ("fusion") of glomerular epithelium. *Lab. Invest.* **36:** 48–61.
22. Blantz, R. C., and C. B. Wilson. 1976. Acute effects of antiglomerular basement membrane antibody on the process of glomerular filtration in the rat. *J. Clin. Invest.* **58:** 899–911.

[8] It is beyond the scope of the present study to explain the mechanism whereby changes in local peritubular capillary Starling forces modulate local net transepithelial fluid absorption. It has been argued that alterations in the peritubular capillary fluid uptake force could influence net transepithelial transport by causing geometrical changes in the adjacent interstitial space (25) or epithelial intercellular channel (26). Such geometrical changes could conceivably bring about local changes in concentration gradients of solutes or in the permeability properties of the apical tight junction (27). It is likely that such geometrical changes accompany local alterations in interstitial hydraulic pressure, P_I (27), or net interstitial pressure, $P_I - \Pi_I$ (28). However, as discussed in footnotes 1 and 2, since these pressures were always <2 mm Hg, changes from one nephron unit to another would escape detection by the methods used.

23. Baylis, C., W. M. Deen, B. D. Myers, and B. M. Brenner. 1976. Effects of some vasodilator drugs on transcapillary fluid exchange in renal cortex. *Am. J. Physiol.* **230:** 1148–1158.
24. Giebisch, G. 1978. The proximal nephron. *In* Physiology of Membrane Disorders. T. E. Andreoli, J. F. Hoffman, and D. D. Fanestil, editors. Plenum Medical Book Co., New York. 629–660.
25. Asteria, M. F., and E. E. Windhager. 1975. Estimate of relative thickness of peritubular interstitial space in *Necturus* kidney. *Am. J. Physiol.* **228:** 1393–1402.
26. Humphreys, M. H., and L. E. Earley. 1971. The mechanism of decreased intestinal sodium and water absorption after acute volume expansion in the rat. *J. Clin. Invest.* **50:** 2355–2367.
27. Stein, J. H., N. H. Lameire, and L. E. Earley. 1978. Renal hemodynamic factors and the regulation of sodium excretion. *In* Physiology of Membrane Disorders. T. E. Andreoli, J. F. Hoffman, and D. D. Fenestil, editors. Plenum Medical Book Co., New York. 739–772.
28. Tucker, B. J., and R. C. Blantz. 1978. Determinants of proximal tubular reabsorption as mechanism of glomerulotubular balance. *Am. J. Physiol.* **235:** F142–F150.